Innate
Immunity

Immunophenotypic, cytotoxic, proteomic and genomic characterization of human cord blood vs. peripheral blood CD56^{Dim} NK cells

Evan Shereck[1],*, Nancy S Day[2],*, Aradhana Awasthi[3],
Janet Ayello[3], Yaya Chu[3], Catherine McGuinn[2],
Carmella van de Ven[3], Megan S Lim[4] and
Mitchell S Cairo[3,5,6,7,8] (iD)

Abstract

Unrelated cord blood (CB) is an excellent alternative as an allogeneic donor source for stem cell transplantation. CB transplantation is associated with lower incidence of severe acute graft versus host disease (GVHD) and chronic GVHD but similar rates of malignant relapse compared with other unrelated donor cell transplants. NK cells are critical innate immune components and the comparison of CB vs. peripheral blood (PB) NK cells is relatively unknown. NK cell receptor expression, cell function, and maturation may play a role in the risk of relapse after CB transplant. We investigated CB vs. PB NK cell subset cytotoxicity, function, receptor expression, and genomic and proteomic signatures. The CB CD56^{dim} compared with PB CD56^{dim} demonstrated significantly increased expression of NKG2A and NKG2D, respectively. CB vs. PB CD56^{dim} NK cells had significantly decreased *in vitro* cytotoxicity against a variety of non-Hodgkin lymphoma targets. Various proteins were significantly under- and over-expressed in CB vs. PB CD56^{dim} NK cells. Microarray analyses and qRT-PCR in CB vs. PB CD56^{dim} demonstrated significantly increased expression of genes in cell regulation and development of apoptosis, respectively. In summary, CB vs. PB CD56^{dim} NK cells appear to be earlier in development, have decreased functional activity, and increased capacity for programmed cell death, suggesting that CB NK cells require functional and maturational stimulation to achieve similar functional levels as PB CD56^{dim} NK cells.

Keywords

Introduction

NK cells comprise approximately 5–15% of circulating lymphocytes and are characterized by expression of CD56 but absence of CD3.[1] NK cells reside in circulating peripheral blood (PB), cord blood (CB), and in

[1]Department of Pediatrics, Oregon Health and Science University, Portland, 97239, USA
[2]Department of Pediatrics, Columbia University, New York, USA
[3]Department of Pediatrics, New York Medical College, Valhalla, USA
[4]Department of Pathology and Laboratory Medicine, University of Pennsylvania, Philadelphia, USA
[5]Department of Medicine, New York Medical College, Valhalla, USA
[6]Department of Pathology, New York Medical College, Valhalla, USA
[7]Department of Microbiology and Immunology, New York Medical College, Valhalla, USA
[8]Department Cell Biology and Anatomy, New York Medical College, Valhalla, USA

*The first two authors contributed equally and are considered co-first authors.

Corresponding author:
Mitchell S Cairo, Maria Fareri Children's Hospital at Westchester Medical Center (WMC), New York Medical College (NYMC), 40 Sunshine Cottage Rd, Skyline 1N-D12, Valhalla, New York 10595, USA.
Email: mitchell_cairo@nymc.edu

various organs such as the lymph nodes, uterus, lung, liver, tonsils, bone marrow (BM), and spleen, and are critical components of the innate host defense against infectious organisms and malignant transformation.[1–8]

The majority (at least 90%) of human PB NK cells express low-density of CD56 (CD56^{dim}) but high levels of Fcγ receptor III (FcγRIII, CD16), whereas about 10% of PB NK cells are CD56^{bright}CD16^{dim} or CD56^{bright}CD16^{−}.[1,9,10] Most CD56^{bright} NK cells are in lymph nodes.[11] The CB CD56^{bright} and CD56^{dim} NK cell subsets are present at about the same proportions as in PB.[12,13] CD56^{dim} CD16^{high} NK cells display significantly higher cytolytic functions than CD56^{bright} cells but low IFN-γ secretion.[9] The CD56^{dim} NK cells mediate direct tumor cytotoxicity through the release of cytotoxic molecules such as perforin and granzyme known as degranulation.[9] Perforin polymerizes and forms the pores in the target cells to facilitate the entry of granzymes and lead to the apoptosis of target cells.[14] Perforin-dependent cytotoxicity is crucial for NK cell-mediated control of tumors.[15] NK cells can also act independently of perforin by NK cell-dependent death receptor-mediated apoptosis.[16] NK cells express FAS (APO-1, CD95) ligand (FasL) and TNF-related apoptosis-inducing ligand (TRAIL/APO-2L).[17] The engagement of the ligands with their corresponding death receptors on tumor targets induces a conformational change in the receptors and recruitment of adaptor protein leading to apoptosis of target cells.[16,18] Upon being activated by target cells, CD56^{dim} NK cells also secrete a wide variety of cytokines such as IFN-γ, TNF-α, GM-CSF, IL-10, IL-5, and IL-13, and chemokines such as MIP-1α, MIP-1β, IL-8, and RANTES to shape the innate and adaptive immune responses.[1,19,20] Additionally, and importantly, CD56^{dim} NK cells often express high level of CD16 and can mediate cytotoxicity through Ab-dependent cellular cytotoxicity (ADCC) through CD16, which binds the Fc portion of Abs to result in NK cell degranulation and perforin dependent target cell lysis.[16]

The CD56^{bright} NK cells are considered "immature" NK cells.[10] These immature or unlicensed NK cells play less of a role in direct cytotoxicity and lack perforin, instead are more responsive to stimulation and respond readily by secreting a variety of cytokines such as IFN-γ when exposed to IL-12, IL-15, and IL-18, which is important in tumor immune surveillance and clearing of infectious pathogens.[9,21,22]

The functions of NK cells are highly regulated by signals through the binding of specific agonists on target cells with the NK repertoire of receptors.[23] The sophisticated network of surface receptors on NK cells can be grouped into activating, inhibitory, adhesion, cytokine, and chemotactic receptors, and are engaged to regulate NK cell functions and to discriminate target cells from healthy "self" cells.[24,25] The activating receptors include the cytotoxicity receptors (NCRs) (NKp46, NKp30, and NKp44), C-type lectin receptors (CD94/NKG2C, NKG2D, NKG2E/H, and NKG2F) and killer cell immunoglobulin-like receptors (KIRs) (KIR-2DS and KIR-3DS), while the inhibitory receptors include C-type lectin receptors (CD94/NKG2A/B) and KIRs (KIR-2DL and KIR-3DL).[26–28] Other modulating co-receptors include members of the signaling lymphocytic activation molecule (SLAM) family, such as 2B4 (CD244), as well as unrelated receptors such as DNAM-1 (CD226), CD2, and NKp80.[27,28] The KIRs and CD94/NKG2 receptors mediate NK cytotoxicity against MHC class I–bearing targets, while NCRs and the NKG2D receptor are important in recognizing tumor cells in an MHC-independent manner.[27,28]

Cairo and others have demonstrated that unrelated CB transplantation (UCBT) is successful in the treatment of malignant and nonmalignant conditions,[29–31] and that the incidence of grade II-IV and grade III-IV acute graft versus host disease (GVHD) and chronic GVHD is significantly lower in UCBT than in matched unrelated adult donor transplantations (MUD).[29,32–35] Interestingly, the rates of malignant relapse following UCBT is still comparable to that reported for MUDs.[36–38]

Ruggeri et al. have demonstrated that following ablative T-cell depleted allogeneic hematopoietic transplants in adults with acute myeloid leukemia (AML), donor/recipient NK receptor/ligand mismatches were associated with a significant improvement in AML disease free survival (0% relapse vs. 75% relapse in KIR mismatch vs. KIR match).[37] The 5-yr overall survival (OS) was 60% in the AML population when KIR mismatch was present compared with 5% with no KIR mismatch.[39] These findings suggest that NK KIR mismatches that favor activation of NK cells may represent an important therapeutic approach. In fact, Verheyden et al. demonstrated that the relapse rate was decreased in patients with AML undergoing human leukocyte Ag (HLA)-identical hematopoietic stem cell transplantation when the donors had two combined specific activating KIRS, KIR2DS1, and KIR2DS2.[39] Given the important role NK cells play in graft-versus-tumor effect and given the increasing use of CB as an allogeneic donor cell source for hematopoietic stem cell transplantation, we compared CB versus adult PB NK cells with respect to characterizing their genomic and proteomic signatures, NKR expression and *in vitro* cytotoxicity.

Materials and methods

NK cell subset isolation

Adult PB was obtained as buffy coat products from healthy adult donors from the New York Blood

Center. Umbilical CB was obtained by venipuncture from umbilical cord veins immediately after infant delivery at Morgan Stanley Children's Hospital of New York-Presbyterian Hospital. This protocol was approved by the Columbia University Human Subjects Institutional Review Board (approval number 0944), and written informed consent was obtained from parents/legal guardians, and patients if over 18 yrs of age, in accordance with the Declaration of Helsinki. PB and CB mononuclear cells (MNC) ($n = 5$ of each) were isolated following Ficoll-Paque (Amersham Biosciences, Piscataway, NJ, USA) density gradient separation. Pure NK cells (CD3$^-$/56$^+$) were isolated by indirect magnetic labeling system with a mixture of biotin-conjugated Abs and the NK Cell MicroBead Cocktail using a standard kit (Miltenyi Biotec, Auburn, CA, USA). After magnetic separation of NK (CD3$^-$/56$^+$) cells, cells were further isolated into CD3$^-$56^{dim} and NK CD3$^-$56^{bright} subsets using a cell sorter (FACS Aria flow cytometer/cell sorter, BD Biosciences, San Jose, CA, USA). After sorting, four distinct NK cell populations were obtained: PB CD56^{dim}/CD16^{bright}, PB CD56^{bright}/CD16^{bright}, CB CD56^{dim}/CD16^{bright}, and CB CD56^{bright}/CD16^{bright}, with 99.9% purity of each subset.

NK receptor expression

NK cell subset populations were analyzed for phenotypic expression of the following NKRs: KIR2DS1 (CD158h), KIR2DL1 (CD158a) and KIR2DL2/L3 (CD158b); activating C-lectin receptors: NKG2D and NKG2C; inhibitory c-type lectin receptor: NKG2a; activating natural cytotoxicity receptors: NKp44 and NKp46; and NKR-P1A (CD161). The sorted NK cell subsets (5×10^5 cells) were washed in PBS supplemented with 10% heat-inactivated FBS and 1% sodium azide (Sigma Aldrich, St. Louis, MI, USA). Fluorescent-conjugated mAbs (CD3, CD56, CD158a, CD158b, CD158h, CD94, NKG2a, NKG2D, NKG2C, Nkp44, and NKp46, and CD161) (BD Biosciences, San Jose, CA, USA and R&D systems, Minneapolis, MN, USA.) were added according to manufacturer directions. Cells were incubated in the dark at 4°C for 30–45 min, washed in azide buffer and fixed with 0.5% paraformaldehyde (Sigma Aldrich). Samples were analyzed on a FACS LSRII (BD Biosciences) flow cytometer. Spectral overlap was electronically compensated using single color controls, and negative gates were set using isotype controls for each experiment. Each NK cell subset was individually analyzed for side and forward scatter and expression of surface Ags recognized by mAbs listed above. A minimum of 10,000 events were collected and analyzed using CellQuest software (BD Biosciences).

Measurement of in vitro *cytotoxicity.* Since there were few CD56^{bright} cells, further studies were performed on PB and CB CD56^{dim} subsets only. Tumor cytotoxicity was compared between PB and CB NK CD56^{dim} against tumor targets as determined by europium release assay (Perkin Elmer, Waltham, MA, USA), as we have described.[40] Tumor cytotoxicity was measured against an anaplastic large cell lymphoma cell line (ALCL), Karpas-299 (DSMZ, Germany), and a diffuse large B-cell lymphoma cell line (DLBCL), Toledo (ATCC, Manhass, VA).

BATDA (acetyoxymethyl ester-enhancing ligand)-labeled tumor targets were re-suspended at a final concentration of 1×10^5 cells/ml. CB and PB NK CD56^{dim} effector cells were added to 5×10^4 labeled tumor targets at varying effector:target (E:T) ratios (5:1, 10:1 and 20:1) for 2 h at 37°C, 5% CO_2. After incubation, cytolytic activity was evaluated using a time-resolved fluorometer (Perkin Elmer, Waltham, MA, USA). Percentage of specific release was calculated as follows:

$$\%\text{Specific release} = \frac{\text{experimental release} - \text{spontaneous release}}{\text{maximum release} - \text{spontaneous release}} \times 100$$

Spontaneous release was determined by incubating tumor targets in medium alone and the maximum release was determined by incubating tumor targets in medium + lysis buffer. Cytotoxicity was expressed as percent specific release. All tests were run in triplicate.

Comparison of CB and PB CD56^{dim} genomics

Total RNA from CB CD56^{dim} and PB CD56^{dim} NK cell subsets were isolated by Trizol reagents (Invitrogen, Carlsbad, CA) and then underwent affinity column purification (Qiagen, Valencia, CA). Subsequent double-stranded complementary deoxyribonucleic acid (cDNA) was generated from 100 ng total RNA using a poly dT oligonucleotide (Affymetrix, Santa Clara, CA), as we have described.[41,42] Biotinylated labeling cRNA was performed by *in vitro* transcription,[41,42] and 15 µg fragmented cRNA was subjected to oligonucleotide hybridization using Fluidics Station 450 (Affymetrix) to human U133A2 gene chip (Affymetrix). The detailed procedures of RNA purification and hybridization for the microarray analyses were as described previously.[41]

To compare CB versus PB CD56^{dim} gene expression, data from the subsets were imported into GeneSpring GX 10 (Agilent Technologies, Foster City, CA) or Partek Genomics Suite (St. Louis, MO), normalized, and presented as log2 values. In GeneSpring, the Welch test was used to perform statistical analysis,

and values of $P < 0.05$ were considered to be significant; 486 genes were identified significantly differentially expressed between CB versus PB CD56^{dim}. The identified gene information and accession numbers were obtained through NetAffx provided by Affymetrix, and further confirmed by a search of GenBank.[43]

Using Affymetrix ID as the identifier, 486 genes were uploaded into the Database for Annotation Visualization and Integrated Discovery (DAVID) at the National Institutes of Health (NIH), and then classified by functional annotation clustering. Each classified group was then re-uploaded into DAVID for further sub-classification.[43,44] In Network Generation Algorithm, pathway interpretation of the 486 genes that had relevance to molecular and cellular functions was generated by Ingenuity Pathways Analysis (IPA 6.5, Redwood City, CA) using the Benjamini-Hochberg multiple testing correction P value. P-Values < 0.03 indicated a statistically significant and non-random association between a set of computational selected genes from the 486 genes and a set of all genes related to a given function in Ingenuity's knowledge base.

Selected genes were examined for their expression levels by real-time quantitative (q)RT-PCR using an RNA One-Step Quantitative RT-PCR System (Invitrogen). Two fluorescence dyes, dye FAM for selected genes and dye JOE for a housekeeping gene, GAPDH, were utilized to measure qRT-PCR products. Passive reference containing dye ROX was used to normalize for non-PCR-related fluctuations in the fluorescence signal. Real-time detection of the RT-PCR product was monitored using ABI7500 (Applied Biosystems, Foster City, CA). Relative quantification (ddCt) of messenger ribonucleic acid (mRNA) expression of each gene was determined by normalizing to the housekeeping gene (GAPDH). cDNA amplification efficiencies of target and reference genes were confirmed to be equivalent and the absolute values of the slope of log input amount vs. ΔC_T were < 0.1.

Comparison of CB and PB CD56^{dim} proteomics

CB and PB CD56^{dim} subsets ($2-5 \times 10^7$ cells) were pelleted from each sample and washed three times using $1 \times$ PBS. Cells were lysed by lysis buffer which contained 100 mM Tris-HCl, pH 8.5, 0.1% SDS and 8 M urea (Sigma, St. Louis, MO). Cell lysates were then homogenized in ice by repeated pipetting followed by microcentrifuge at high speed for 15 min at 4°C, and the supernatants were collected for further proteomic study. Protein concentrations were determined using the Bradford assay, as described.[43,44]

Approximately 100 μg of protein for each sample was precipitated in ice-cold acetone at –20°C for 2 h.

Proteins were dissolved, denatured, and cysteines were blocked. iTRAQ^{TM} labeling and two-dimensional (2D) liquid chromatrography were performed.[43–48] The mixture was collected by centrifugation, washed, and the proteins were digested with trypsin, mixed with the isobaric tagging iTRAQ^{TM} reagents, and analyzed with SEQUEST, ProteinProphet, and INTERACT. The peptides were resolved by 2D liquid chromatographic separation technique. MS/MS spectra were acquired using an Orbitrap XL Tandem Mass Spectrometer (ThermoFisher, Pittsburgh, PA). MS/MS data was searched using X!Tandem/TPP software against human IPI database (v3.50) appended with decoy sequences. iTRAQ^{TM} ratios of proteins (ProteinProphet probability of > 0.9) were normalized and differentially expressed proteins were selected for further analysis.[45,47]

Peptide identifications were performed using the X! Tandem algorithm. Each MS/MS spectrum was searched against a database of human protein sequences from the National Cancer Institute. Only peptides with a confidence interval $> 90\%$ were retained for further analysis, and a false discovery ratio (FDR) < 0.4 was considered significant. Accurate peptide identification took into consideration the peptide charge state, the number of unique peptides per protein, and the delta correlation score from the next nearest hit. The Ingenuity and GoMiner software programs assisted data analysis and heat map expression profiles were produced with the MultiExperiment Viewer 4.4 using an optimized hierarchical clustering program.[46]

Two-color ECL Plex fluorescence western blotting (WB) was performed to validate the proteomic data. Total proteins (50–100 μg) were suspended in Laemmli sample buffer, boiled, and subjected to SDS-PAGE on 10% gels. Proteins were transferred to polyvinylidene difluoride membranes by electroblotting and the membranes were incubated in primary Ab with 2% blocking agent overnight. The membranes were incubated with a GAPDH Ab for an additional 2 h the next day followed by incubation with Cyanine 5 (CY5)- and Cyanine 3 (CY3)-conjugated immunoglobulin G (IgG) (1:5000, GE HealthCare, Pittsburgh, PA) for 1 h. Blots were scanned using TYPHOON TRIO by green (532 laser and 580 filter) and red (633 laser and 670 filter) setting for CY3 and CY5, respectively, and analyzed using ImageQuant.

Functional interpretation of the significantly altered expressed genes or proteins between CB vs. PB CD56^{dim} NK cells and their relevance to molecular and cellular functions and pathways was generated by Ingenuity gene/protein interaction knowledge base (http://www.ingenuity.com) (IPA 6.5, Redwood City, CA); $P < 0.05$ indicated statistical significance.

Statistical analyses

Statistical differences between two groups were analyzed by Student *t*-test, and differences between multiple groups were analyzed by one-way analysis of variance (ANOVA) followed by the Tukey multiple comparison test. Results are expressed as mean $\pm$ SEM with $P \leq 0.05$ considered significant.

Results

NKR phenotype characterization in PB versus CB CD56^{dim} and CD56^{bright} NK cells

We first characterized PB and PB $CD56^{dim}/CD16^{bright}$, PB $CD56^{bright}/CD16^{bright}$, CB $CD56^{dim}/CD16^{bright}$, and CB $CD56^{bright}/CD16^{bright}$, populations (Figure 1a–d). The PB $CD56^{dim}$ versus PB $CD56^{bright}$ demonstrated significantly increased expression of KIR2DL1 (30.85 ± 5.02 vs. $3.52 \pm 1.05\%$, $P = 0.03$) and KIR2DL1/KIR2DS1 (31.76 ± 2.85 vs. $7.62 \pm 1.99\%$, $P = 0.006$). The PB $CD56^{bright}$ versus PB $CD56^{dim}$ cell had significantly increased expression of NKG2A (96.13 ± 0.97 vs. $54.09 \pm 4.56\%$, $P < 0.01$) and NKG2D (94.45 ± 2.21 vs. $77.43 \pm 3.93\%$, $P = 0.03$).

The CB $CD56^{dim}$ cell subset demonstrated significantly increased expression versus the CB $CD56^{bright}$ in KIR2DL2 (31.88 ± 4.39 vs. 3.08 ± 0.99, $P < 0.02$).

The CB $CD56^{dim}$ compared with PB $CD56^{dim}$ demonstrated significantly increased expression of NKG2A (81.34 ± 1.51 vs. $54.09 \pm 4.56\%$, $P < 0.03$) (Figure 1e) and NKG2D (94.08 ± 2.36 vs. $77.43 \pm 3.93\%$, $P < 0.035$), respectively (Figure 1d). There was no significant difference in NKR expression between the PB $CD56^{bright}$ and the CB $CD56^{bright}$ subsets.

Tumor target cytotoxicity

Mean cytotoxicity was significantly decreased in CB $CD56^{dim}$ ($n = 3$) vs. PB $CD56^{dim}$ ($n = 3$) subsets with DLBCL tumor targets (Toledo) at all E:T ratios (E:T 5:1: 5.86 ± 0.6 vs. 21.3 ± 2, $P < 0.001$; 10:1: 15.1 ± 1.3 vs. 40 ± 1.4, $P < 0.001$; 20:1: 42 ± 2.1 vs. $59.8 \pm 1.3\%$, $P < 0.01$). Likewise, mean cytotoxicity of CB ($n = 3$) vs. PB $CD56^{dim}$ ($n = 3$) subsets with Karpas (ALCL) tumor targets at 5:1, 10:1, and 20:1 E:T ratios were also significantly decreased (5.7 ± 0.82 vs. 11.3 ± 1.5, $P < 0.01$; 12.5 ± 1.5 vs. 20.24 ± 1.8, $P < 0.01$; 29.9 ± 2.1 vs. 44.7 ± 3.6, $P < 0.01$, respectively).

Functional groups of differentially over-expressed proteins in CB vs. PB CD56^{dim} NK cells

The proteins over-expressed in CB *vs.* PB $CD56^{dim}$ cells represent multiple functional categories that include roles in binding (22%), catalytic activity (28%),
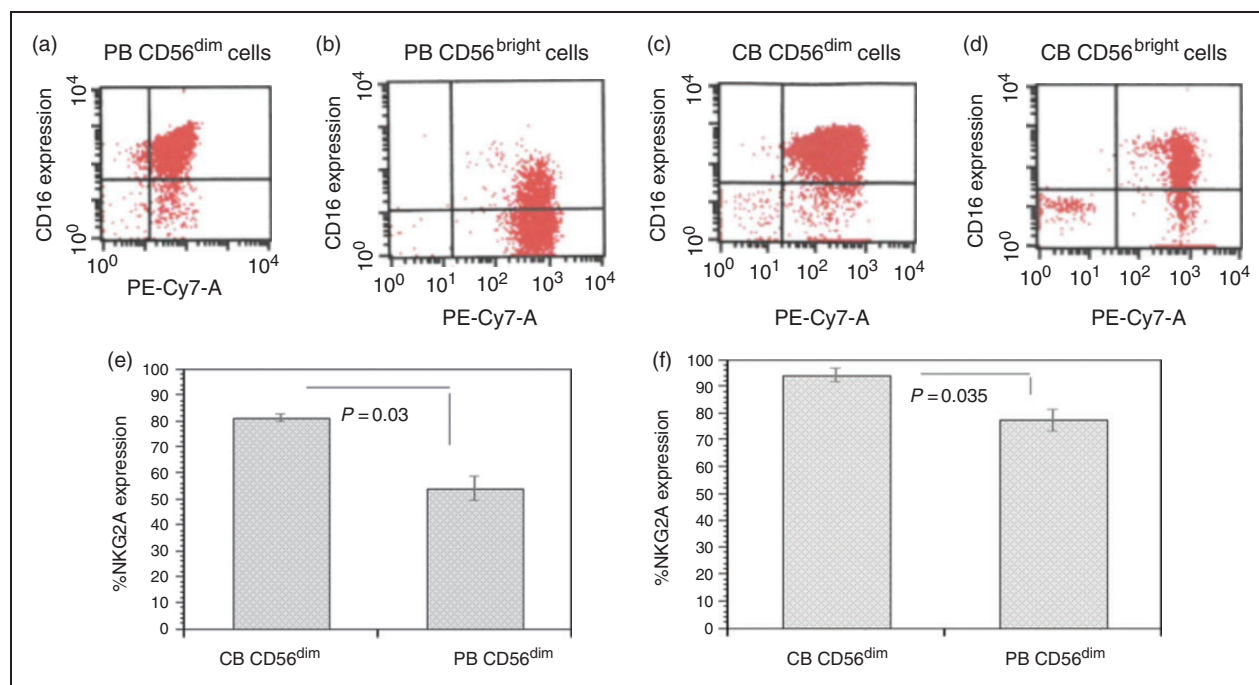

Figure 1. Characterization of PB and CB $CD56^{dim}/CD16^{bright}$, $CD56^{bright}/CD16^{bright}$, populations and receptor expression of CB NK $CD56^{+dim}$ compared with PB $CD56^{+dim}$ NK cells. Flow cytometry histogram of PB $CD56^{dim}/CD16^{bright}$ (a), PB $CD56^{bright}/CD16^{bright}$ (b), CB $CD56^{dim}/CD16^{bright}$ (c), and CB $CD56^{bright}/CD16^{bright}$ (d) populations. When compared with PB $CD56^{+dim}$, CB $CD56^{+dim}$ demonstrated a significant increased expression of NKG2A ($P < 0.03$, e) and NKG2D ($P < 0.035$, f). $n = 5$.
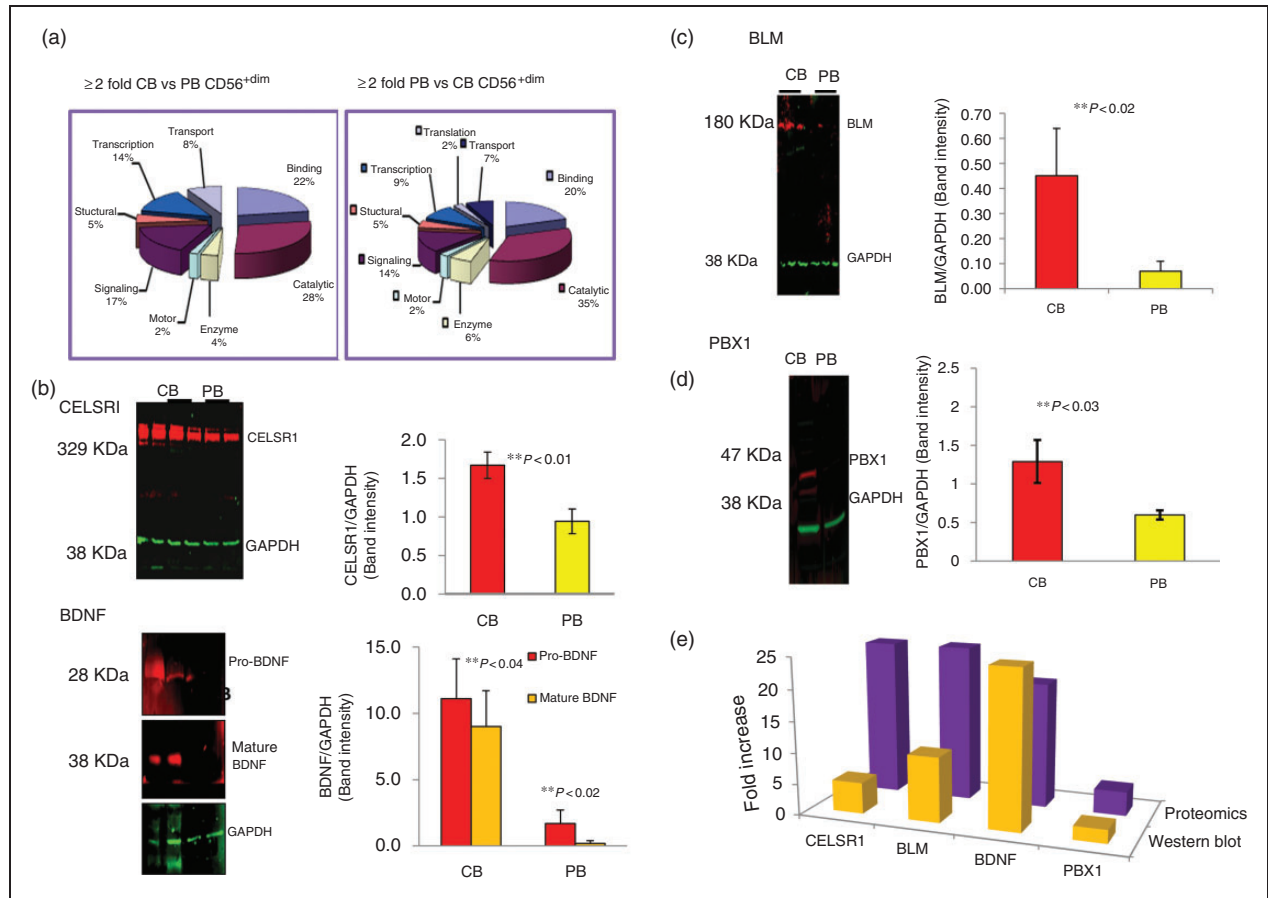
Figure 2. Difference in protein content between CB CD56^{+dim} vs. PB CD56^{+dim} NK cells by quantitative analysis using iTRAQ^{TM} labeling and 2D liquid chromatography. (a) $\geq$ 2-Fold expression of CB vs. PB CD56^{dim} and PB vs. CB CD56^{dim} ($n = 5$). (b) Significant up-regulation of CELSR1 and BDNF binding proteins ($n = 5$). (c) Significant up-regulation of developmental proteins BLM ($n = 5$) by functional category. (d) Significant up-regulation of developmental proteins PBX1 ($n = 5$). (e) Comparison of proteomics and Western blot analysis of signaling proteins CELSR1, BLM, BDNF, and PBX1 ($n = 5$).

signaling (17%), transcription (14%), structure (5%), motor (2%), as well as enzymes (4%) (Figure 2a). PB vs. CB CD56^{dim} cells demonstrated significantly over-expression of ion channel protein (HCN4; 33.3F), organic anions transporter (SO1C1; 20.0F), bM specific protein (MEPE; 33.3F), actin cytoskeleton regulator (DIAP2; 20.0F), among others (Table 1).

Western blot analysis corroborates MS-based quantitative proteomics in CB versus PB CD56^{dim} NK cells

Selective proteins that were found to be over-expressed in the proteomic study were analyzed by WB. We observed complete concordance in the trends of differential expression of the proteins in the proteomics and WB results. CELSR1, BDNF, BLM, and PBX1 (pre-B-cell leukemia transcription factor 1, 3.9-fold increase, as shown in Table 1) (Figure 2b–e) were up-regulated in CB versus PB CD56^{dim} subsets. We also

identified a zinc finger group of five proteins, ZN155 (2.3F), ZN212 (5.3F), GAK8 (12.5F), ESR2 (2.4F), and NFX1 (5.3F), that were down-regulated in CB CD56^{dim} NK cells.

CB versus PB CD56^{dim} protein pathway and function analysis

Depicting the diverse signaling pathways affected by CB vs. PB CD56^{dim} NK cells, IPA results demonstrated the top molecular functions of these proteins including gene expression ($P < 0.03$), apoptosis ($P < 0.03$), and cellular development ($P < 0.03$). CELSR1, BDNF, ESR2, TAGLN, SIRT2, PBX1, and AIFM1, together with HOX variants, FOXA1, FOS, and SP1, facilitate in part a cell developmental network (Supplemental Figure 1). NOTCH2, BDNF, PKD1, LETM1, AIFM1, SIRT2, ESR2, and EP400 together with cMYC, NF-kB, and TP53, build, in part, a network toward apoptotic activity.

Table 1. Significantly over-expressed proteins in PB vs. CB CD56^{dim} cells.

Uniprot	Accession	Protein description	Fold increase[a]
CELSR1	Q9NYQ6	Cadherin EGF LAG seven-pass G-type receptor 1 precursor	25.00
BLM	P54132	Bloom syndrome protein	25.00
LGP2	Q96C10	ATP-dep helicase; innate immune defense	25.00
TR95	Q9Y2X0	Thyroid hormone receptor-associated protein complex 95 kDa component	20.00
BDNF	P23560	Brain-derived neurotrophic factor precursor	20.00
PKD1	P98161	Polycystin-1 precursor	16.67
NOTCH2	Q04721	Neurogenic locus notch homolog protein 2 precursor	16.67
AGGF1	Q8N302	Angiogenic factor with G patch and FHA domains 1	16.67
BIRC2	Q13490	Baculoviral IAP repeat-containing protein 2	12.50
GAK8	Q9HDB9	HERV-K_3q12.3 provirus ancestral Gag polyprotein	12.50
PDCD8	O95831	Programmed cell death protein 8, mitochondrial precursor; AIFM1	12.50
GP73	Q8NBJ4	Golgi phosphoprotein 2	12.50
MEPE	Q9NQ76	Bone marrow specific protein	33.33
HCN4	Q9Y3Q4	Potassium/sodium hyperpolarization-activated cyclic nucleotide-gated channel 4	33.33
DIAP2	O60879	Protein diaphanous homolog 2	20.00
SO1C1	Q9NYB5	Solute carrier organic anion transporter family member 1C1	20.00
CD2L7	Q9NYV4	Cell division cycle 2-related protein kinase 7	12.50
KCRB	P12277	Energy homeostasis; CKB; creatinine kinase B-type	12.50
SIN3A	Q96ST3	Paired amphipathic helix protein Sin3a	12.50
SMCA5	O60264	SWI/SNF-related matrix-associated actin-dependent regulator of chromatin	11.11
IF3X	O75153	Putative eukaryotic translation initiation factor 3 subunit	10.00
MTERF	Q99551	Transcription termination factor, mitochondrial precursor	8.33

[a]Fold increase in peripheral blood versus cord blood protein expression.

Differential gene expression of CB versus PB CD56^{dim}

Based on the difference in expression, we identified shared and distinct groups of up- and down-regulated genes in CB vs. PB CD56^{dim} cells. CB vs. PB CD56^{dim} cells had significantly altered expression of 796 genes, in which 486 genes with 8 major functions were over expressed (Figure 3a,b). The most common functions were transmembrane genes (38%), regulation of transcription genes (18%), adenyl ribonucleotide binding genes (15%), cytoskeleton genes (4%), GTPase regulator activity genes (2%), ubiquitin-like conjugation pathway genes (2%), translation regulation genes (2%), and apoptosis genes (1%) (Supplemental Figure 2). Furthermore, the transmembrane genes were involved in cell development and other signal transduction pathways. The regulation of transcription group is involved with transcription factor and DNA binding and zinc fingers activities. The genes in the adenyl ribonucleotide binding group are involved in cell cycling, microtubule motor, and protein kinase activities.

Five pro-apoptotic genes were identified to be over expressed in CB^{dim} vs. PB^{dim} (Figure 3c). The genes that were significantly under-expressed in CB^{dim} vs. PB^{dim} (Figure 3d) included: *JUN*(–2.2F), *BAX*(–2.9F), *NF1*(–5.1F) and *PI3K*(–2.1F), and additional genes that were significantly over-expressed were: *PBX1* (7.6F), *IL1RN*(5.1F), *CD24*(5.3F), *CD34*(3.5F), *CD55*

(2.2F), and *CCL13*(2.2F), respectively (Figure 3d). Of all the over-expressed genes, the largest functional group contained genes involved in the regulation of cell growth, signaling and apoptosis. Ingenuity™ pathways analysis confirmed these results (Supplemental Figure 1).

Real-time qRT-PCR

To further confirm the differential expression of genes revealed by cDNA microarray analysis, we analyzed the expression of *CD34*, which was over expressed in CB^{dim} vs. PB^{dim} (Figure 3d), by real-time qRT-PCR (Figure 4a). The qRT-PCR analysis of CD34 demonstrated high concordance with the results of the genomic analysis in CB vs. PB CD56^{dim} NK cells (Figure 4b). Overall, there was approximately 50% similarity between the microarray results and the qRT-PCR results.

Discussion

Our research adds to the body of literature on the characterization of NK subsets in PB and CB. While our research reinforces findings from previous studies, we have the unique perspective of combining our phenotype work with proteomics and genomics results. Our genomics, in particular, leads to some explanation of
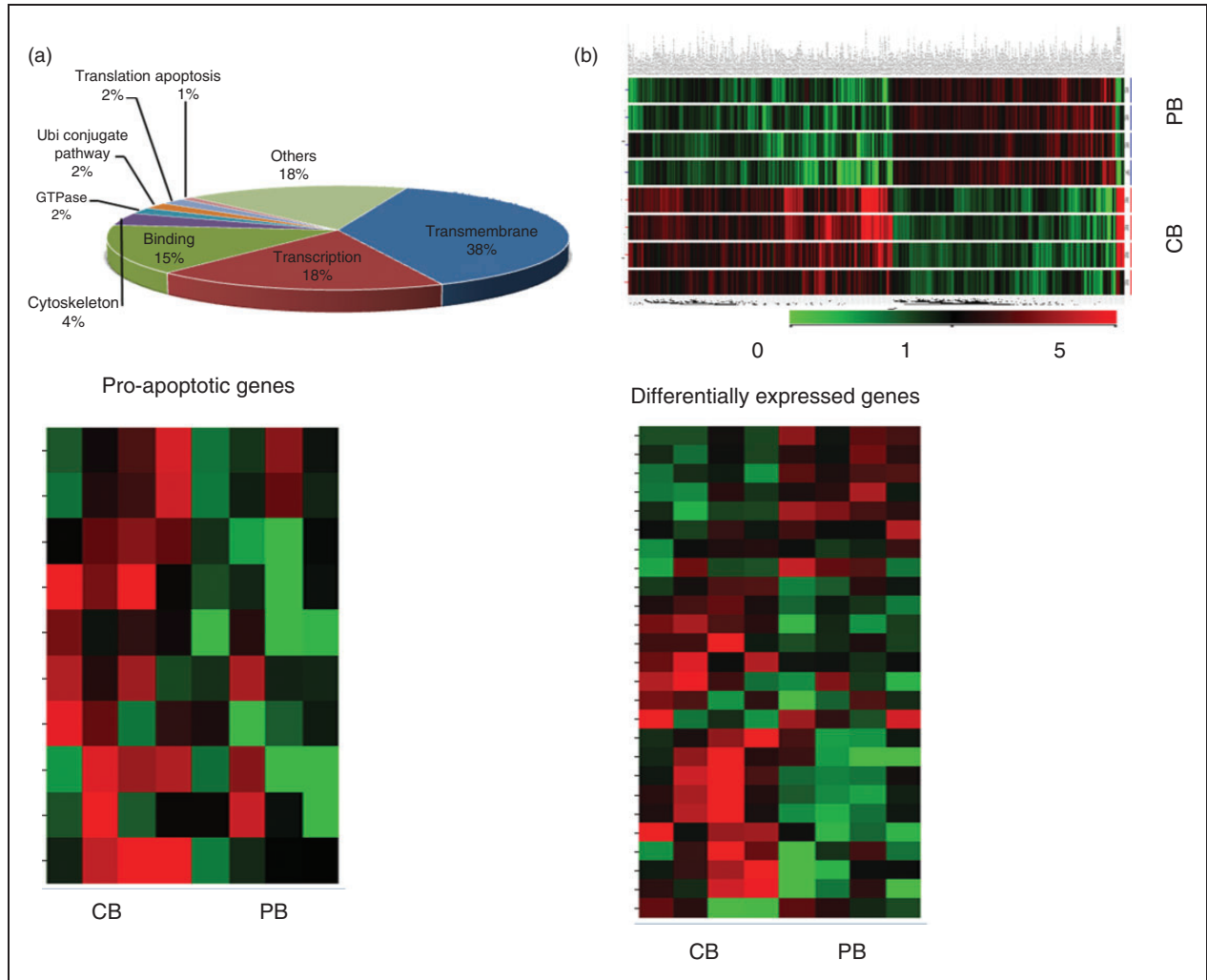
Figure 3. Gene expression profiles of CB CD56^{+dim} vs. PB CD56^{+dim} NK cells. (a) Representative pie chart showing gene functions that were over-expressed when comparing CB CD56^{+dim} vs. PB CD56^{+dim} NK cells. This included transmembrane genes (38%), transcription regulation genes (18%), adenyl ribonucleotide binding genes (15%), cytoskeleton (4%), GTPase regulator activity (2%), ubiquitin-like conjugation pathway (2%), translation regulation (2%), and apoptosis (1%) ($n = 5$); (b) Gene expression signature of CB CD56^{+dim} vs. PB CD56^{+dim} NK cells ($n = 5$); (c) Representative sample of differentially expressed genes that were over-expressed NOTCH2 (1.5F), CASP10 (3.1F), TNFSF11 (4.7F), CDC2 (3.0F), and BCL2L1(4.3F) when comparing CB CD56^{+dim} vs. PB CD56^{+dim} NK cells ($n = 5$); (d) Representative sample of 10 differentially expressed genes, of which 4 were under-expressed, JUN (–2.2F), BAX (–2.9F), NF1 (–5.1F) and PI3K (–2.1F), and 6 were over-expressed PBX1 (7.6F), IL1RN (5.1F), CD24 (5.3F), CD34 (3.5F), CD55 (2.1F), and CCL13 (2.2F) when comparing CB CD56^{+dim} vs. PB CD56^{+dim} NK cells ($n = 5$).

why the maturity of the NK cell affects their genetic expression, which in turn affects cytotoxicity.

Interestingly, while CB CD56^{bright} and PB CD56^{bright} did not differ in their NK cell receptor expression, CB CD56^{dim} and PB CD56^{dim} differed by CB CD56^{dim} having increased expression of NKG2A and NKG2D. This has been corroborated by other studies that have also demonstrated greater expression of NKG2A in CB CD56^{dim} and equal expression of KIR receptors among CB CD56^{dim} and PB CD56^{dim}.[12,13,49] Based on these results, it would appear that, in part, CB CD56^{dim} may be more

mature than the CB CD56^{bright} but perhaps less mature than the PB CD56^{dim}, similar to descriptions by others.[12,50,51]

We and others have shown that the percentages of CB vs. PB CD56^{dim} and CD56^{bright} remains consistent regardless of the source (CB or PB).[12,13] While cytotoxicity was increased in both PB and CB CD56^{dim} NK subsets with increasing E:T ratios against DLBCL and ALCL tumor targets, the CB CD56^{dim} NK cells exhibited significantly less cytolytic capacity compared with PB CD56^{dim} NK cells, as has been previously described against K562 targets.[49,52,53] However, after exposure to
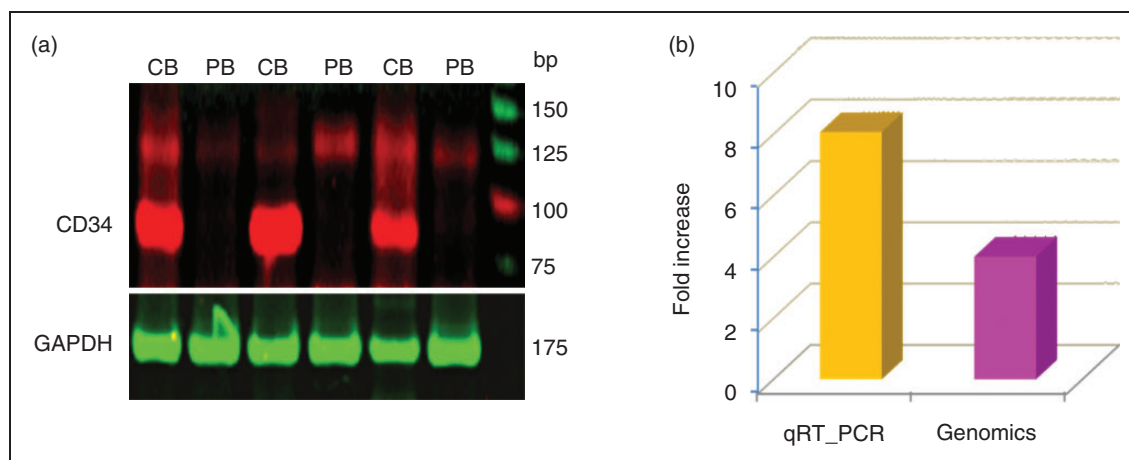
Figure 4. Differential expression of CD34 gene by (a) quantitative fluorescent real-time PCR (qRTPCR) and the (b) qRT-PCR vs. microarray of CB CD56^{+dim} vs. PB CD56^{+dim} NK cells ($n = 3$).

certain cytokines, CB NK cells can rapidly increase cytotoxicity.[12,13,53,54] Since the tumor targets used in this study express Class I, and, given the small sample size and lack of measurement of C1, C2, Bw4 expression in the tumor targets used for the study, licensing of NK cells could be a confounding factor.

We demonstrated that the purified CB CD56^{dim} cells over-express CD34 compared with PB CD56^{dim} cells. This indicates that CB CD56^{dim} cells may be earlier in development (pro-NK) compared with their PB counterparts.[51] In addition, CB vs. PB CD56^{dim} NK cells are also more prone to undergo programmed cell death (apoptosis) secondary to over-expression of numerous pro-apoptotic genes. In fact, the brain derived neurotrophic factor (*BDNF*) gene has been shown to have a high affinity to TrkB (a tyrosine kinase) and binding of BDNF to TrkB leads to apoptosis.[55,56] The CB CD56^{dim} subset also had increased neurogenic locus homolog protein 2 (NOTCH2) expression, which can lead to apoptosis.[57] Lastly, since NKG2D-mediated cytotoxicity is PI-3 kinase dependent, the low PI-3 kinase content in CB CD56^{dim} observed in our study may further explain the lower cytotoxic ability in CB CD56^{dim}.

We observed 84 under-expressed and 102 over-expressed proteins in CB vs. PB CD56^{dim} by proteomic analysis. This includes a number of functional proteins like binding, catalytic, enzyme, motor, signaling, structural, transcription, and translation proteins. We demonstrated that CB CD56^{dim} significantly over express early developmental stage proteins (CELSR1,[57] BLM,[58] BDNF, and PBX1, pre-B-cell acute lymphoblastic leukemia[16]), apoptotic proteins (PKD1, NOTCH2, AGGF1, BIRC2, AIFM1), and an innate immune defense protein (LGP2). These findings support the hypothesis that CB CD56^{dim} may be less mature than the PB CD56^{dim} subsets.

In summary, our studies demonstrate that CB CD56^{dim} cells are significantly immature, have less *in vitro* cytotoxicity against tumor targets, and over-express pro-apoptotic genes and genes early in development compared with PB CD56^{dim} NK cell subsets. These studies suggest that functional activation and maturation of CD56^{dim} NK cells by the local microenvironment cytokine milieu are critical for their function and efficacy post-UCBT. Further studies are required to better delineate the signaling pathways that are specifically altered in CB CD56^{dim} vs. PB CD56^{dim} and determine the mechanisms for enhanced functional activation and maturation.

ORCID iD

Mitchell S Cairo ![ORCID] https://orcid.org/0000-0002-2075-434X

Supplemental material

Supplemental material is available for this article online.

References

1. Freud AG, Mundy-Bosse BL, Yu J, et al. The broad spectrum of human natural killer cell diversity. *Immunity* 2017; 47: 820–833.
2. Melsen JE, Lugthart G, Vervat C, et al. Human bone marrow-resident natural killer cells have a unique transcriptional profile and resemble resident memory CD8(+) T cells. *Front Immunol* 2018; 9: 1829.
3. Lugthart G, Melsen JE, Vervat C, et al. Human lymphoid tissues harbor a distinct CD69+CXCR6+ NK cell population. *J Immunol* 2016; 197: 78–84.
4. Aw Yeang HX, Piersma SJ, Lin Y, et al. Cutting edge: human CD49e- NK cells are tissue resident in the liver. *J Immunol* 2017; 198: 1417–1422.
5. Cooper GE, Ostridge K, Khakoo SI, et al. Human CD49a(+) Lung natural killer cell cytotoxicity in response to influenza A virus. *Front Immunol* 2018; 9: 1671.
6. Montaldo E, Vacca P, Chiossone L, et al. Unique eomes(+) NK cell subsets are present in uterus and decidua during early pregnancy. *Front Immunol* 2015; 6: 646.
7. Strowig T, Brilot F, Arrey F, et al. Tonsilar NK cells restrict B cell transformation by the Epstein-Barr virus via IFN-gamma. *PLoS Pathog* 2008; 4: e27.
8. Witte T, Wordelmann K and Schmidt RE. Heterogeneity of human natural killer cells in the spleen. *Immunology* 1990; 69: 166–170.
9. Cooper MA, Fehniger TA and Caligiuri MA. The biology of human natural killer-cell subsets. *Trends Immunol* 2001; 22: 633–640.
10. Poli A, Michel T, Thérésine M, et al. CD56bright natural killer (NK) cells: an important NK cell subset. *Immunology* 2009; 126: 458–465.
11. Sarvaria A, Jawdat D, Madrigal JA, et al. Umbilical cord blood natural killer cells, their characteristics, and potential clinical applications. *Front Immunol* 2017; 8: 329.
12. Verneris MR and Miller JS. The phenotypic and functional characteristics of umbilical cord blood and peripheral blood natural killer cells. *Br J Haematol* 2009; 147: 185–191.
13. Dalle JH, Menezes J, Wagner E, et al. Characterization of cord blood natural killer cells: implications for transplantation and neonatal infections. *Pediatr Res* 2005; 57: 649–655.
14. Topham NJ and Hewitt EW. Natural killer cell cytotoxicity: how do they pull the trigger? *Immunology* 2009; 128: 7–15.
15. Osińska I, Popko K and Demkow U. Perforin: an important player in immune response. *Cent Eur J Immunol* 2014; 39: 109–115.
16. Shereck E, Satwani P, Morris E, et al. Human natural killer cells in health and disease. *Pediatr Blood Cancer* 2007; 49: 615–623.
17. Zamai L, Ahmad M, Bennett IM, et al. Natural killer (NK) cell-mediated cytotoxicity: differential use of TRAIL and Fas ligand by immature and mature primary human NK cells. *J Exp Med* 1998; 188: 2375–2380.
18. Screpanti V, Wallin RP, Ljunggren HG, et al. A central role for death receptor-mediated apoptosis in the rejection of tumors by NK cells. *J Immunol* 2001; 167: 2068–2073.
19. Vivier E, Tomasello E, Baratin M, et al. Functions of natural killer cells. *Nat Immunol* 2008; 9: 503–510.
20. Fauriat C, Long EO, Ljunggren HG, et al. Regulation of human NK-cell cytokine and chemokine production by target cell recognition. *Blood* 2010; 115: 2167–2176.
21. Lieberman LA and Hunter CA. Regulatory pathways involved in the infection-induced production of IFN-gamma by NK cells. *Microbes Infect* 2002; 4: 1531–8.
22. Shankaran V, Ikeda H, Bruce AT, et al. IFNgamma and lymphocytes prevent primary tumour development and shape tumour immunogenicity. *Nature* 2001; 410: 1107–1111.
23. Lanier LL. NK cell recognition. *Ann Rev Immunol* 2005; 23: 225–274.
24. Raulet DH and Vance RE. Self-tolerance of natural killer cells. *Nat Rev Immunol* 2006; 6: 520–531.
25. Vivier E, Raulet DH, Moretta A, et al. Innate or adaptive immunity? The example of natural killer cells. *Science* 2011; 331: 44–49.
26. Cheng M, Chen Y, Xiao W, et al. NK cell-based immunotherapy for malignant diseases. *Cell Mol Immunol* 2013; 10: 230–252.
27. Long EO, Kim HS, Liu D, et al. Controlling natural killer cell responses: integration of signals for activation and inhibition. *Annu Rev Immunol* 2013; 31: 227–258.
28. Handgretinger R, Lang P and André MC. Exploitation of natural killer cells for the treatment of acute leukemia. *Blood* 2016; 127: 3341–3349.
29. Cairo MS and Wagner JE. Placental and/or umbilical cord blood: an alternative source of hematopoietic stem cells for transplantation. *Blood* 1997; 90: 4665–4678.
30. Kurtzberg J, Laughlin M, Graham ML, et al. Placental blood as a source of hematopoietic stem cells for transplantation into unrelated recipients. *New Engl J Med* 1996; 335: 157–166.
31. Wagner JE, Rosenthal J, Sweetman R, et al. Successful transplantation of HLA-matched and HLA-mismatched umbilical cord blood from unrelated donors: analysis of engraftment and acute graft-versus-host disease. *Blood* 1996; 88: 795–802.
32. Cairo MS, Rocha V, Gluckman E, et al. Alternative allogeneic donor sources for transplantation for childhood diseases: unrelated cord blood and haploidentical family donors. *Biol Blood Marrow Transplant* 2008; 14: 44–53.
33. Geyer MB, Jacobson JS, Freedman J, et al. A comparison of immune reconstitution and graft-versus-host disease following myeloablative conditioning versus reduced toxicity conditioning and umbilical cord blood transplantation in paediatric recipients. *Br J Haematol* 2011; 155: 218–234.
34. Rubinstein P, Carrier C, Scaradavou A, et al. Outcomes among 562 recipients of placental-blood transplants from unrelated donors. *New Engl J Med* 1998; 339: 1565–1577.

35. Styczynski J, Cheung YK, Garvin J, et al. Outcomes of unrelated cord blood transplantation in pediatric recipients. *Bone Marrow Transplant* 2004; 34: 129–136.

36. Klingebiel T, Reinhardt D, Bader P, et al. Place of HSCT in treatment of childhood AML. *Bone Marrow Transplant* 2008; 42 Suppl 2: S7–S9.

37. Ruggeri L, Capanni M, Urbani E, et al. Effectiveness of donor natural killer cell alloreactivity in mismatched hematopoietic transplants. *Science* 2002; 295: 2097–2100.

38. Szabolcs P and Cairo MS. Unrelated umbilical cord blood transplantation and immune reconstitution. *Semin Hematol* 2010; 47: 22–36.

39. Verheyden S, Schots R, Duquet W, et al. A defined donor activating natural killer cell receptor genotype protects against leukemic relapse after related HLA-identical hematopoietic stem cell transplantation. *Leukemia* 2005; 19: 1446–1451.

40. Ayello J, van de Ven C, Cairo E, et al. Characterization of natural killer and natural killer-like T cells derived from ex vivo expanded and activated cord blood mononuclear cells: implications for adoptive cellular immunotherapy. *Exp Hematol* 2009; 37: 1216–1229.

41. Jiang H, van de Ven C, Baxi L, et al. Differential gene expression signatures of adult peripheral blood vs. cord blood monocyte-derived immature and mature dendritic cells. *Exp Hematol* 2009; 37: 1201–1215.

42. Jiang H, Van De Ven C, Satwani P, et al. Differential gene expression patterns by oligonucleotide microarray of basal versus lipopolysaccharide-activated monocytes from cord blood versus adult peripheral blood. *J Immunol* 2004; 172: 5870–5879.

43. Deffenbacher KE, Iqbal J, Sanger W, et al. Molecular distinctions between pediatric and adult mature B-cell non-Hodgkin lymphomas identified through genomic profiling. *Blood* 2012; 119: 3757–3766.

44. Lim MS, Carlson ML, Crockett DK, et al. The proteomic signature of NPM/ALK reveals deregulation of multiple cellular pathways. *Blood* 2009; 114: 1585–1595.

45. Ashburner M, Ball CA, Blake JA, et al. Gene ontology: tool for the unification of biology. The Gene Ontology Consortium. *Nat Genet* 2000; 25: 25–29.

46. Feng X, Zhang J, Chen WN, et al. Proteome profiling of Epstein-Barr virus infected nasopharyngeal carcinoma cell line: identification of potential biomarkers by comparative iTRAQ-coupled 2D LC/MS-MS analysis. *J Proteomics* 2011; 74: 567–576.

47. Lund TC, Anderson LB, McCullar V, et al. iTRAQ is a useful method to screen for membrane-bound proteins differentially expressed in human natural killer cell types. *J Proteome Res* 2007; 6: 644–653.

48. Wallentine JC, Kim KK, Seiler CE 3rd, et al. Comprehensive identification of proteins in Hodgkin lymphoma-derived Reed-Sternberg cells by LC-MS/MS. *Lab Invest* 2007; 87: 1113–1124.

49. Wang Y, Xu H, Zheng X, et al. High expression of NKG2A/CD94 and low expression of granzyme B are associated with reduced cord blood NK cell activity. *Cell Mol Immunol* 2007; 4: 377–382.

50. Luetke-Eversloh M, Killig M and Romagnani C. Signatures of human NK cell development and terminal differentiation. *Front Immunol* 2013; 4: 499.

51. Yu J, Freud AG and Caligiuri MA. Location and cellular stages of natural killer cell development. *Trends Immunol* 2013; 34: 573–582.

52. Luevano M, Daryouzeh M, Alnabhan R, et al. The unique profile of cord blood natural killer cells balances incomplete maturation and effective killing function upon activation. *Hum Immunol* 2012; 73: 248–257.

53. Tanaka H, Kai S, Yamaguchi M, et al. Analysis of natural killer (NK) cell activity and adhesion molecules on NK cells from umbilical cord blood. *Eur J Haematol* 2003; 71: 29–38.

54. Lin SJ and Yan DC. ICAM-1 (CD54) expression on T lymphocytes and natural killer cells from umbilical cord blood: regulation with interleukin-12 and interleukin-15. *Cytokines Cell Mol Ther* 2000; 6: 161–164.

55. Tejeda GS and Diaz-Guerra M. Integral characterization of defective BDNF/TrkB signalling in neurological and psychiatric disorders leads the way to new therapies. *Int J Mol Sci* 2017; 18.

56. Yang B, Qin J, Nie Y, et al. Brain-derived neurotrophic factor propeptide inhibits proliferation and induces apoptosis in C6 glioma cells. *Neuroreport* 2017; 28: 726–730.

57. Aoyama K, Delaney C, Varnum-Finney B, et al. The interaction of the Wnt and Notch pathways modulates natural killer versus T cell differentiation. *Stem Cells* 2007; 25: 2488–2497.

58. Chu Y, Hochberg J, Yahr A, et al. Targeting CD20+ aggressive B-cell non-Hodgkin Lymphoma by anti-CD20 CAR mRNA-modified expanded natural killer cells in vitro and in NSG mice. *Cancer Immunol Res* 2015; 3: 333–344.